

Fast Registration of Intraoperative Ultrasound and Preoperative MR Images Based on Calibrations of 2D and 3D Ultrasound Probes

Fang Chen¹, Ruizhi Liao¹ and Hongen Liao^{1*}

¹ Department of Biomedical Engineering, School of Medicine, Tsinghua University, Beijing 100084, China

Abstract—During the intraoperative-ultrasound-guided intervention, ultrasound (US) is often registered with other high-quality preoperative images like computed tomography (CT) or magnetic resonance (MR) to improve the navigation accuracy. However, real-time registration is difficult to achieve due to the difference of image modality and dimensionality. To solve this problem, we apply preoperative 3D US image collected with a 3D calibrated probe to simplify 2D US and 3D MR image registration into two easy-achieved steps: 2D-3D US intra-modal registration and 3D US 3D MR pre-operative registration. To achieve fast intraoperative 2D US and preoperative 3D US registration, we take advantage of effective 2D and 3D US probes' calibration results and get a near optimal registration transform. Then intraoperatively we just need to do an automatic local adjustment, which will make real-time registration become possible. To achieve effective calibrations, we design an improved calibration phantom and propose a warm-start iterative closest points (ICP) method.

Keywords—calibration, registration, ultrasound guidance

I. INTRODUCTION

US image is commonly used in minimally invasive surgery navigation due to its real-time imaging capabilities. Due to the limit of image quality, intraoperative 2D US is often fused with preoperative MR or CT to provide more effective navigation information. US has been recognized as a promising method for quantifying and correcting brain shift in neurosurgery [1]. During US-guided liver intervention, registration between preoperative CT and intraoperative US can improve the accuracy of the guidance [2].

Many registration approaches between CT/MR and US based on image similarity measures such as the sum square difference (SSD), mutual information (MI), and correlation ratio (CR) have been proposed [3]. However current researches are difficult to achieve fast and accurate registration to satisfy clinical demand. Preoperative calibration of US probe is widely used for registration during ultrasound-guided surgery [2]. But current researches focus on just using 2D or 3D US probe calibration alone for registration and navigation. For 2D US probe's calibration, one of the popular methods is N-wire phantom [4]. For 3D US probe's calibration, Poon *et al.* compares three calibration phantoms, namely IXI-wire, stylus and cube and find IXI-wire phantom achieves the best result [5]. There are a few of reports about 3D calibration in recent literatures.

In this paper, we utilize effective 2D and 3D US probes' calibration results to achieve real-time registration between 2D US and 3D MR. Moreover, to simplify 3D US probe's calibration we propose a warm-start ICP method. In our registration method, most of the steps are done preoperatively and intraoperatively with just an automatic local registration adjustment, 2D US can be registered to 3D MR.

II. MATERIALS AND METHODS

A. Registration procedure and experiment platform

The procedure of proposed registration of intraoperative US and preoperative MR images based on 2D and 3D US probes' calibrations is shown in Fig. 1a. When operation begins, we employ a calibrated 3D probe to acquire 3D US image of target organ and record 3D probe's pose in tracking system. This step is done just one time and the collected data is used to align preoperative 3D US with intraoperative 2D US.

To get a near-optimal start value of registration transform T_{2DUS}^{3DUS} , we need 2D and 3D US probes' calibration results and 3D pose information of 2D and 3D US probes. On the one hand, with the calibrations of 2D and 3D US probes we can get the transform $T_{2DUS}^{S_{2D}}$ from intraoperative 2D US coordinate to 2D probe sensor coordinate S_{2D} and the transform $T_{3DUS}^{S_{3D}}$ from preoperative 3D US to 3D probe sensor coordinate S_{3D} . Details about US probe's calibration are provided in Section B. On the other one hand, by applying a tracking system to record the 3D pose of intraoperative 2D US probe and preoperative 3D US probe, we can acquire the transform $T_{S_{2D}}^{TS}$ from 2D US probe sensor coordinate S_{2D} to tracking system coordinate TS and the transform $T_{S_{3D}}^{TS}$ from 3D probe sensor coordinate S_{3D} to tracking system coordinate TS . Finally, the near-optimal start value of registration transform T_{2DUS}^{3DUS} can be computed by

$$T_{2DUS}^{3DUS} = T_{2DUS}^{S_{2D}} * T_{S_{2D}}^{TS} * \left(T_{S_{3D}}^{TS}\right)^{-1} * \left(T_{3DUS}^{S_{3D}}\right)^{-1} \quad (1)$$

With the acquired near-optimal start transform, we employ an automatic intensity-based local registration adjustment to achieve accurate intraoperative registration T_{2DUS}^{3DUS} between intraoperative 2D US and preoperative 3D US.

For preoperative registration between 3D US and 3D MR images, we use manual registration method. Then the dual-

modality registration T_{2DUS}^{3DMR} between intraoperative 2D US and preoperative 3D MR images can be calculated by

$$T_{2DUS}^{3DMR} = T_{2DUS}^{3DUS} * T_{3DUS}^{3DMR} \quad (2)$$

Our experiment platform includes an US system, an optical tracking system and a heart phantom (Fig. 1b). US images are collected with the US system (iU22 xMATRIX, Philips) using a linear array probe (VL13-5) and a phased array probe (S5-1). The probes are tracked by an optical tracking system (Polaris, Northern Digital Inc), with passive optical markers attached. A realistic environment is simulated using a MR compatible multi-modality heart phantom (SHELLEY Medical, USA), which contains left ventricular (LV) and right ventricular (RV) and coronary artery (CA).

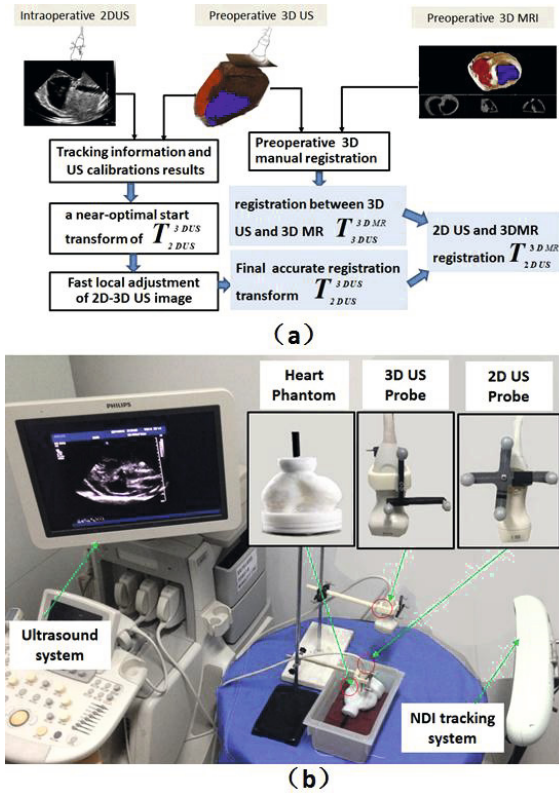


Fig. 1(a) Registration procedure between 2D US and 3D MR images. (b) Experimental system: Tracking system, US system and a heart phantom.

B. 2D and 3D US probes' calibrations for a near-optimal start value of registration T_{2DUS}^{3DUS}

To realize fast and accurate registration between 2D and 3D US, a near-optimal start transform is crucial. And this near-optimal start value needs 2D US and 3D US probes' calibration results. So in this section, we will introduce the details of calibration. Firstly the calibration procedure and the designed calibration phantom will be introduced. Com-

pared with 2D US probe's calibration, 3D US probe's calibration is more challenging. How to align 3D calibration phantom's physical coordinate with calibration phantom's US image coordinate is a key step for 3D calibration. And we propose a warm-start ICP method to solve this problem.

a) Calibration procedure and calibration phantom

There are four main transforms in calibration procedure for both 2D and 3D US probes. (1) T_{TS}^S Transform from tracking system coordinate (TS) to probe sensor coordinate (S); (2) T_{TS}^P Transform from tracking system coordinate to calibration phantom's physical coordinate (P); (3) T_{US}^P Transform from US image coordinate to calibration phantom's physical coordinate; (4) T_{US}^S Transform from US image coordinate to probe sensor coordinate. The calibration transform T_{US}^S can be computed by

$$T_{US}^S = T_{US}^P * (T_{TS}^P)^{-1} * T_{TS}^S \quad (3)$$

By 2D and 3D US calibrations, transform $T_{2DUS}^{S_{2D}}$ from 2D US coordinate to 2D probe sensor coordinate S_{2D} and transform $T_{3DUS}^{S_{3D}}$ from 3D US to 3D probe sensor coordinate S_{3D} can be achieved with Equ.3. These calibration results can be used to get a near optimal registration start value of T_{2DUS}^{3DMR} .

We design an applicative calibration phantom (length: 26 cm width: 12 cm height: 28 cm), which is suit for both 2D and 3D US probes' calibrations. For 2D US probe's calibration, our phantom use traditional N-wire. It contains four layers and each layer has two N-wires of different sizes (Fig. 2a). For 3D US probe's calibration we create an improved phantom with two kinds of IXI-wires on four layers (Fig. 2b). The IXI-wire is created by adding a wire to N-wire of the 2D phantom. This phantom has more asymmetry information than the phantom Poons *et al.* [5] proposed and can achieve a good registration result.

b) Using warm-start ICP method to solve T_{US}^P

There are two point sets P_p under 3D calibration phantom's physical coordinate and P_{US} under calibration phantom's 3D US image coordinate are generated. P_p (The red point on left image of Fig. 2c) is generated by a uniform sampling from calibration phantom. P_{US} (The green point on the right image of Fig. 2c) is obtained by sampling uniformly from those voxels above 90% of the max gray value of calibration phantom's US volume.

Traditional ICP method is sensitive to the initial positions and easy to be trapped at a local optimal solution [6]. Such cases will occur (The left image of Fig. 2d) if we use traditional ICP method to align P_{US} with P_p . To address this problem, we propose a warm-start ICP method. The warm-start ICP is carried out as follows:

(1) A nearly-omni-direction rotation matrix group $R_k (k=1 \dots m)$ is created based on Rodrigues' rotation formula.

This rotation matrix group covers the range of 3D rotation uniformly.

(2) The US point set P_{US} is preprocessed using the generated rotation matrix group R_k to get different processed point clouds P_k by $P_k = R_k * P_{US}$ ($k=1 \dots m$).

(3) Point sets P_k and P_p are aligned using traditional ICP method and a group of rotation R'_k ($k=1 \dots m$), corresponding translation T'_k ($k=1 \dots m$) and the different Euclidean distance error E'_k ($k=1 \dots m$) are acquired.

(4) The min Euclidean error E'_j and its corresponding rotation R'_j , translation T'_j and the created rotation R_j in step (1) for processing are found. Final rotation between P_{US} and P_p is $R = R'_j * R_j$ and translation is $T = T'_j$.

Using proposed warm-start ICP, we can easily and effectively achieve the correct registration of points under US volume coordinate and phantom coordinate (The right image of Fig. 2d) and determine the coordinate transform T_{US}^p .

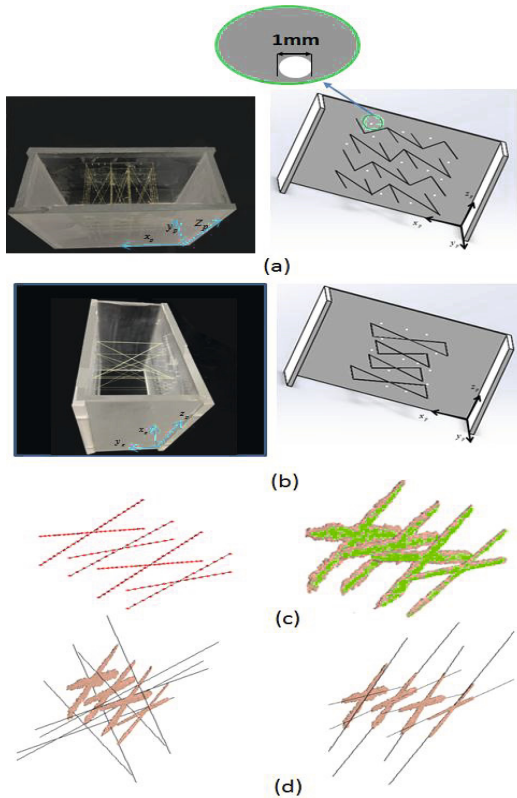


Fig. 2 Calibration phantoms and results. (a) 2D US calibration phantom. Left: actual phantom. Right: design drawing. (b) 3D US calibration phantom. Left: actual phantom. Right: design drawing. (c) Two point sets P_p and P_{US} . Left image: selected phantom feature point set (red points) on the physical phantom (black line) Right image: selected US feature point sets (green points) on the 3D US (brown volume) of the IXI-wire phantom. (d) Registration result. Left image: registration between physical phantom (black line) and US volume (blown volume) using traditional ICP method. Right image: registration result using warm-start ICP method.

There are 25 positioning holes (depth: 1mm diameter: 1mm) distributing on the calibration phantom (Fig. 2a). By recording these holes' positions under phantom's physical coordinate and tracking system coordinate, we can get two 3-D point sets. Using the method Arun *et al* [7] proposed, transform T_{TS}^p can be solved. In addition, depending on 3D pose of the probe sensor in tracking system coordinate, we can get transform T_{TS}^s from tracking system coordinate to probe sensor coordinate. Then we can compute calibration transform T_{US}^s with Equ.3.

C. Intensity-based intraoperative local adjustment

With 2D and 3D US probe calibration results, a near optimal registration transform between intraoperative 2D US and pre-operative 3D US is achieved. To make registration more accurate, intensity-based intraoperative local adjustment is needed. For local adjustment, MI method is implemented with gradient ascent algorithm doing optimization.

III. CALIBRATION AND REGISTRATION RESULTS

A. Calibration error evaluation

During several calibration trials, T_{US}^s transform from US image coordinate to US probe sensor coordinate should yield a same result. To get an accurate calibration transform, we use average value of acquired Euler angle around x, y and z axes in several calibration trials to represent the rotation of final calibration transform. We use the average value of acquired translation value around x, y and z axes to represent the translation of final calibration transform. To evaluate the reproducibility of calibration results, we define the rotation reproducibility error E_{eu} and translation reproducibility error E_t , as

$$E_{eu} = \sum_{i=1}^N \|eu_i - \overline{eu}\| / N \quad (4)$$

$$E_t = \sum_{i=1}^N \|t_i - \bar{t}\| / N$$

where N is the number of calibration trials, eu_i and t_i mean acquired Euler angle and translation in i th calibration trial, \overline{eu} and \bar{t} mean average Euler angle and translation. In addition, we also evaluated calibrations' reconstruction accuracy. The reconstruction accuracy evaluation method is proposed by Bergmeir *et al.* [8]. During the evaluations of 2D and 3D probes' calibration, we both performed 8 calibration trials, using 10 images per trial, 80 datasets in total. The calibration's reproducibility error is shown in Table 1. The 2D probe calibration's reconstruction error is 2.61mm. Our calibration reconstruction error of 3D US probe is 3.97mm, which is similar to 3.3mm Bergmeir *et al.* acquired [8].

Table 1 Reproducibility error of 2D and 3D probes' calibrations

	Axis	2D US calibration	3D US calibration
Translation (mm)	x	0.37	0.68
	y	0.42	0.57
	z	0.51	0.43
Rotation ($^{\circ}$)	x	0.28	0.35
	y	0.46	0.37
	z	0.78	0.15

B. Registration result of heart phantom study

We firstly registered 3D US volume and 2D US image of heart phantom using 2D and 3D US probes' calibration results. The contour of the ventricle in 3D US acquired a near-optimal agreement with ventricle edge in 2D US image (Fig. 3a). So calibration results are effective and a near-optimal registration can be acquired. To achieve more accurate registration, we added intensity-based local adjustment and performed registration for 2D-3D US images of heart phantom. The ventricle in 3D US was registered to corresponding ventricle edge in 2D US image and a better agreement can be seen in Fig. 3b. Finally, by adding manual registration result between 3D US and 3D MR images, heart phantom's 2D US were fused with 3D MR images (Fig. 3c).

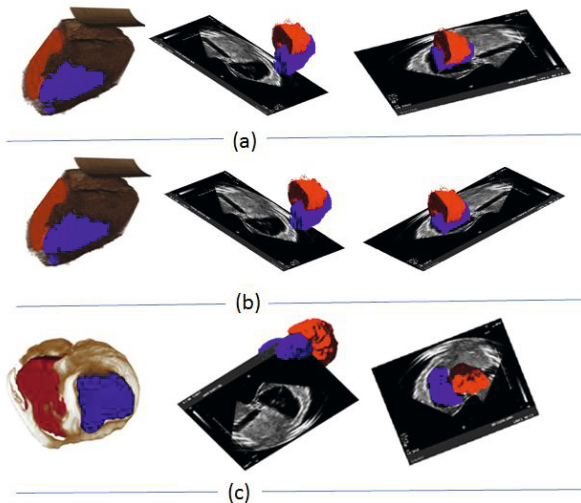


Fig. 3 registration results. (a) Registration using calibrations' results. left: 3D US image of heart phantom (red volume is LV, blue is RV), middle: 2D US and 3D US image before registration, right: Registration using calibrations' results. (b) Registration after a local adjustment. left: 3D US image, middle: 2D US and 3D US images before registration, right: registration results. (c) 2D US 3D MR registration results. left: 3D MR image of heart phantom (red volume is LV, blue is RV), middle: 2D US and 3D MR images before registration, right: 2D US and 3D MR registration results.

IV. DISCUSSION AND CONCLUSION

We present an intraoperative 2D US and preoperative 3D MR image registration method based on the calibrations of 2D and 3D US probes. The calibration reconstruction accuracy of 2D US probe is 2.61mm, and of 3D US probe is 3.97mm. In cardiac phantom registration experiment, ventricle in 2D US can acquire a good agreement with corresponding ventricle edge in 3D MR images. Results show our proposed method can achieve registration between intraoperative US and preoperative 3D MR images. In the future, we will perform quantitative registration accuracy evaluation experiment, and apply our proposed registration method to beating heart phantom. Our registration method takes advantage of effective 2D 3D US probes' calibration results and just needs to do an automatic local adjustment intraoperatively. Thus, it has the potential to satisfy clinical demand in US guided intervention surgery.

ACKNOWLEDGMENT

The authors thank the support of National Natural Science Foundation of China (Grant No. 81271735, 61361160417, 81427803) and Grant-in-Aid of Project 985.

REFERENCES

1. Comeau, R. M *et al.* (2000). Intraoperative ultrasound for guidance and tissue shift correction in image-guided neurosurgery. *Medical Physics*, 27(4), 787-800.
2. Xu, L. *et al.* (2013). A novel algorithm for CT-ultrasound registration. In *Point-of-Care Healthcare Technologies* (pp. 101-104).
3. Markelj, P *et al.* (2012). A review of 3D/2D registration methods for image-guided interventions. *Medical image analysis*, 16(3), 642-661.
4. Pagoulatos, N *et al.* (2001). A fast calibration method for 3-D tracking of ultrasound images using a spatial localizer. *Ultrasound in medicine & biology*, 27(9), 1219-1229.
5. Poon, T. C., & Rohling, R. N. (2007). Tracking a 3-D ultrasound probe with constantly visible fiducials. *Ultrasound in medicine & biology*, 33(1), 152-157.
6. Besl, P. J., & McKay, N. D. (1992, April). Method for registration of 3-D shapes. In *Robotics-DL tentative* (pp. 586-606).
7. Arun, K. S *et al.* (1987). Least-squares fitting of two 3-D point sets. *Pattern Analysis and Machine Intelligence, IEEE Transactions on*, (5), 698-700.
8. Bergmeir, C *et al.* (2009). Comparing calibration approaches for 3D ultrasound probes. *International journal of computer assisted radiology and surgery*, 4(2), 203-213.

Author: Hongen Liao
 Institute: Department of Biomedical Engineering, School of Medicine, Tsinghua University
 Street: 1 Qinghuayuan, Haidai District,
 City: Beijing
 Country: China
 Email: liao@tsinghua.edu.cn